Electric-field-induced strain effects on the magnetization of a $Pr_{0.67}Sr_{0.33}MnO_3$ film

Bangmin Zhang,[1,2] Cheng-Jun Sun,[3] Weiming Lü,[2] T. Venkatesan,[1,2,4,5] Myung-Geun Han,[6] Yimei Zhu,[6] Jingsheng Chen,[1,*] and Gan Moog Chow[1,*]

[1]*Department of Materials Science and Engineering, National University of Singapore, 117576, Singapore*

[2]*NUSNNI-Nanocore, National University of Singapore, 117411, Singapore*

[3]*Advanced Photon Source, Argonne National Laboratory, Argonne, Illinois 60439, USA*

[4]*Department of Physics, National University of Singapore, 117542, Singapore*

[5]*Department of Electrical and Computer Engineering, National University of Singapore, 117576, Singapore*

[6]*Condensed Matter Physics and Materials Science, Brookhaven National Laboratory, Upton, New York 11973, USA*

(Received 11 March 2015; revised manuscript received 28 April 2015; published 26 May 2015; corrected 8 October 2015)

The electric-field control of magnetic properties of $Pr_{0.67}Sr_{0.33}MnO_3$ (PSMO) film on piezoelectric $Pb(Mg_{1/3}Nb_{2/3})O_3 - PbTiO_3$ (PMNT) substrate was investigated. The piezoelectric response of the PMNT substrate to the electric field produced strain that was coupled to the PSMO film. The in-plane compressive (tensile) strain increased (decreased) the magnetization. The change of magnetic moment was associated with the Mn ions. First-principles simulations showed that the strain-induced electronic redistribution of the two e_g orbitals ($3d_z^2$ and $3d_{x^2-y^2}$) of Mn ions was responsible for the change of magnetic moment. This work demonstrates that the magnetoelectric effect in manganite/piezoelectric heterostructures originates from the change in e_g orbital occupancy of Mn ions induced by strain rather than the interfacial effect.

DOI: 10.1103/PhysRevB.91.174431 PACS number(s): 68.35.−p, 75.70.−i, 75.85.+t, 77.65.−j

I. INTRODUCTION

The demand to develop materials with new multifunctional capabilities has stimulated significant interests in multiferroics, which is characterized by the coexistence of, and coupling between, magnetic and electric order parameters [1,2]. Due to the weak coupling between magnetic and electric ordering in single-phase multiferroic materials [3], investigations on ferromagnetic/ferroelectric (or dielectric) heterostructures have attracted much attention. The coupling mechanisms in the heterostructure are classified into several categories [4], i.e., charge-based coupling [5], elastic [6], and magnetic exchange bias [7]. In the charge-based coupling, the electron accumulation/depletion at an interface under the electric field caused the change of number of electrons in $3d$ orbitals of magnetic atoms which altered magnetic properties such as magnetic anisotropy [8], Curie temperature, and magnetic moment [9,10]. This interfacial magnetoelectric effect has been applied to spin torque transfer magnetic random memory to reduce the switching current [11,12]. In elastic-based coupling, the magnetoelectric effect was enhanced in the heterostructure by using magnetic material with a large magnetostrictive coefficient and ferroelectric material with a large piezoelectric coefficient. Giant electric-field tuning of magnetic properties has been reported in the FeGaB/lead zinc niobate-lead titanate heterostructure [13,14].

Enhanced elastic coupling was also found in another kind of heterostructure $Re_{1-x}A_xMnO_3$/ferroelectric, where Re is a trivalent rare earth element and A is a divalent metal. Electric-field modulation of Curie temperature, magnetization of mixed-valence manganites has been reported in $La_{0.8}Sr_{0.2}MnO_3/Pb(Zr_{0.2}Ti_{0.8})O_3$ [4,15], $La_{0.7}A_{0.3}MnO_3$ (A = Sr,Ca) / $Pb(Mg_{1/3}Nb_{2/3})_{0.72}Ti_{0.28}O_3$ [6,16–20], $Pr_{0.6}Ca_{0.4}MnO_3/Pb(Mg_{1/3}Nb_{2/3})_{0.7}Ti_{0.3}O_3$ [21], and $Pr_{0.5}Sr_{0.5}MnO_3/Pb(Mg_{1/3}Nb_{2/3})_{0.67}Ti_{0.33}O_3$ [22]. The magnetoelectric coupling may be explained by the following two mechanisms. One is due to the strong electron-phonon coupling [6]. The strain induced by the piezoelectric substrate under the electric field changed the Mn-O-Mn bond length and bond angle due to the Jahn-Teller effect and octahedral rotation [23], which caused the change of magnetic properties dominated by double exchange coupling. The other one is due to the interfacial effect [9], i.e., the accumulation/depletion of free carriers to screen the bound charges at the surface of ferroelectric substrates. The accumulation/depletion of free carriers caused the change of the magnetic phase of mixed-valence manganites, for example, changing from ferromagnetic coupling to antiferromagnetic coupling at the interface [4,10]. The interfacial contribution to the effects of electric field on manganite films is less significant in thick films, thus allowing the film properties to be probed without complication of anomalous interfacial effects.

The study of the effects of electric field on properties of $Pr_{0.7}Sr_{0.3}MnO_3$ (PSMO, bulk $T_c \sim 300$ K) with a smaller bandwidth than $La_{0.7}Sr_{0.3}MnO_3$ and a larger bandwidth than $La_{0.7}Ca_{0.3}MnO_3$ is limited. In this paper, we demonstrate the tuning of magnetization of 140-nm-thick PSMO film in PSMO/PMNT heterostructure by electric field at different temperatures. The large film thickness was chosen to minimize interfacial effects. The electric-field-induced strain was an effective way to control magnetic properties in a wide temperature range. The observed magnetization of PSMO film showed a clear dependence on applied electric field. X-ray magnetic circular dichroism (XMCD) results showed that the change of magnetic moment with electric field was due to the strain-induced electronic redistribution in Mn ion rather than the interfacial effects. First-principles calculations revealed that the lattice strain in PSMO caused electronic redistribution among the two e_g suborbitals ($3d_z^2$ and $3d_{x^2-y^2}$). The change in e_g orbital occupancy was responsible for the observed change in magnetic moment. This work presents an example of correlation of lattice strain with orbital occupancy

*Corresponding authors: msecj@nus.edu.sg; msecgm@nus.edu.sg

in mixed-valence manganite films under electric-field-induced strain in magnetoelectric heterostructures.

II. EXPERIMENTAL

The 140-nm-thick $Pr_{0.67}Sr_{0.33}MnO_3$ (PSMO) film was deposited on the (001) $Pb(Mg_{1/3}Nb_{2/3})O_3 - PbTiO_3$ (PMNT) single-crystal substrate using pulsed laser deposition at substrate temperature of 630 °C and oxygen pressure of 100 mTorr. This thickness was chosen to study the electron-phonon coupling and minimize interfacial effects. The electron microscopy work was performed at the Brookhaven National Laboratory, USA. X-ray diffraction (XRD) of the PSMO/PMNT heterostructure was conducted using a Bruker D8 x-ray diffractometer equipped with Cu K_{α_1} radiation. For *in situ* XRD θ - 2θ scan, the electric field was applied on the PMNT substrate with 2θ from 44° to 50° at room temperature. The resistance of the PMNT substrate was estimated to be larger than $1 \times 10^9\ \Omega$ at room temperature using a Keithley 2410 multimeter source. In order to improve the contact, 5-nm Au films were deposited on both sides of the sample as electrodes. The magnetic moment was measured using a superconducting quantum interference device (SQUID) and XMCD. The XMCD at the $\boldsymbol{L}_{3,2}$ edges of Mn and $\boldsymbol{M}_{5,4}$ edges of Pr were measured with an applied in-plane magnetic field of 5000 Oe, conducted at beamline 4-ID-C at the Advanced Photon Source (APS) in Argonne National Laboratory (ANL) using reflectivity mode [24] at 80 K.

III. RESULTS AND DISCUSSION

An illustration of sample configuration with electric field and applied magnetic field is shown in the Supplemental Material (SM) S1 [25]. Figure 1(a) shows the selected-area electron diffraction of the PSMO/PMNT system. From the measured d spacing, the calculated out-of-plane lattice constant of PSMO film was 3.857 Å and the in-plane lattice constant was 3.868 Å. Compared to the lattice constant of bulk PSMO (3.860 Å) and PMNT (4.032 Å), the PSMO film was partially strained by the underlying PMNT substrate. When the electric field (E) was applied along the [001] direction of the PMNT substrate, the out-of-plane lattice constant $\boldsymbol{c}$ of PMNT at room temperature was roughly linearly dependent on the E field [Fig. 1(b)]. Cycling the $\boldsymbol{E}$ field from positive (pointing to the PSMO film) to negative direction (pointing to the PMNT substrate), a butterflylike hysteresis loop typical for the converse piezoelectric effect [26] with coercive field ~3 kV/cm was observed [$\boldsymbol{E}_{cn}$ and $\boldsymbol{E}_{cp}$ in Fig. 1(b)], which is consistent with the reported results for a PMNT single crystal [6]. The direction of the electric field and induced strain are shown in Fig. 1(b), insets (1)–(4). The value of $\boldsymbol{c}$ increased by 0.17% [right axis in Fig. 1(b)], with $\boldsymbol{E} = +10$ kV/cm compared to that without electric field. This resulted in the decrease of in-plane lattice constant by 0.08% under the assumption of volume conservation (S2 in SM) [16,27]. The upper inset of Fig. 1(b) shows an example of a θ - 2θ XRD scan of the PSMO/PMNT heterostructure with and without applied $\boldsymbol{E}$ field. An applied $\boldsymbol{E}$ field of 6.7 kV/cm shifted the PSMO (002) peak to a lower angle, increasing the $\boldsymbol{c}$ value of PSMO film from 3.857 to 3.861 Å. The increase of $\boldsymbol{c}$ in PSMO followed the contraction of the in-plane lattice of PSMO (and PMNT substrate) under $\boldsymbol{E}$ field because of the epitaxial relationship of PSMO/PMNT (S3 in SM).

The PSMO film was paramagnetic at room temperature, and the paramagnetic-ferromagnetic phase transition occurred at ~220 K (S4 in SM). Figure 2 shows the in-plane and out-of-plane $\boldsymbol{M}$-$\boldsymbol{H}$ loops measured at 100 K using SQUID.

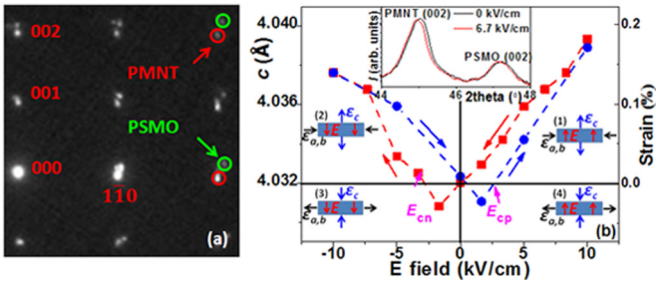

FIG. 1. (Color online) (a) Selected area electron diffraction of PSMO/PMNT heterostructure without electric field; (b) dependence of the out-of-plane lattice constant of PMNT substrate on electric field. Upper inset: the θ - 2θ curves of PSMO/PMNT system with/without electric field; insets (1)-(4) indicate the direction of electric field, in-plane, and out-of-plane strain.

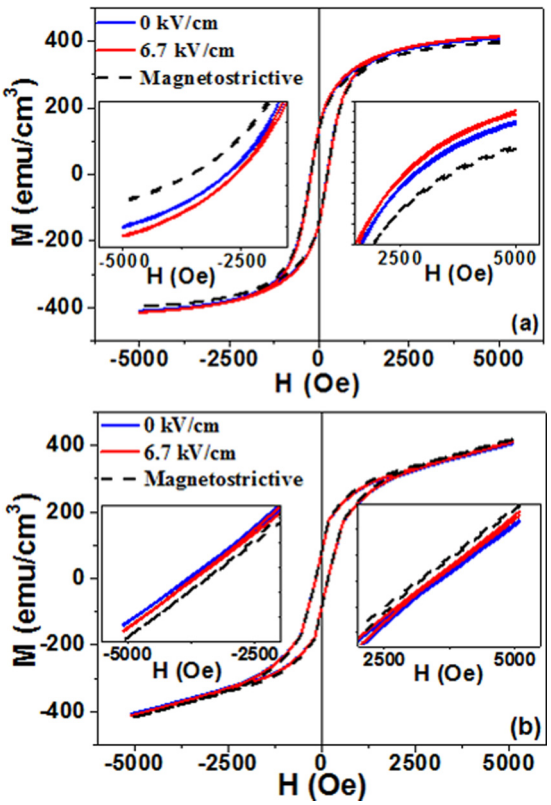

FIG. 2. (Color online) (a) In-plane and (b) out-of-plane M-H curves of PSMO/PMNT with electric field +6.7 kV/cm at 100 K. The insets are the enlarged view of the M-H curves. The black dashed line in each figure illustrates the magnetostriction effect with $E = 6.7$ kV/cm, which induced magnetic anisotropy ~140 Oe perpendicular to the film plane and reduced the in-plane moment and increased the out-of-plane moment with constant magnetic field.

The inset shows the enlarged part of M-H loops clearly, indicating that both the in-plane and out-of-plane magnetic moments increased with applied +6.7 kV/cm. It is well known that strain can change the magnetization due to the magnetostriction effect. The magnetostriction energy [28] is

$$E_\lambda = -3\lambda\sigma\cos^2\alpha/2, \quad (1)$$

where α is the angle between the stress and the magnetization moment, λ the magnetostriction coefficient $\sim 2.5 \times 10^{-5}$ [29], and σ the stress. The in-plane lattice constant for bulk PSMO is 3.860 Å. For the PSMO film deposited on PMNT, the in-plane lattice constant of the PSMO film was 3.868 Å (due to the larger in-plane constant of bulk PMNT 4.032 Å). The PSMO film was under tensile strain compared to its bulk counterpart. When an $\boldsymbol{E}$ field was applied, the in-plane lattice constants of both PSMO and PMNT decreased. At $\boldsymbol{E} = 6.7$ kV/cm, the in-plane lattice constant of PSMO decreased from 3.868 to 3.865 Å. Therefore, the in-plane tensile strain of PSMO in the PSMO/PMNT heterostructure decreased with applied $\boldsymbol{E}$ field. The decrease of in-plane tensile strain tends to rotate the magnetic easy axis of the induced magnetostriction anisotropy from the in-plane to the out-of-plane direction [30–32]. As discussed in S5 in the SM, for $\boldsymbol{E} = 6.7$ kV/cm the induced magnetic anisotropy was ~140 Oe, perpendicular to the film plane. Accordingly, if induced magnetostriction was significant, the out-of-plane magnetic moment should therefore increase with applied $\boldsymbol{E}$ at a constant magnetic field [as indicated by the black dashed line in Fig. 2(b)]. On the other hand, the in-plane magnetic moment should decrease or at least remain constant [as indicated by the black dashed line in Fig. 2(a)]. However, the experimentally observed increased moment [red line in Fig. 2(a)] with applied $\boldsymbol{E}$ contradicted the expected effect of magnetostriction. This suggests that factors other than magnetostriction must be considered.

To understand the anomalous behavior of in-plane magnetic moment, the effects of electric poling (polarization) on magnetization at low temperature were investigated [Fig. 3(a)]. During the measurement, the positive field +6.7 kV/cm was first applied on the PMNT substrate at room temperature, and then the sample was cooled down to 100 K in the absence of magnetic field. The magnetization was then measured under different applied $\boldsymbol{E}$. The reversible change of magnetization with respect to the zero-electric-field reference showed an opposite trend for the positive and the negative $\boldsymbol{E}$ field. With an $\boldsymbol{E}$ field of +6.7 kV/cm, the magnetization increased by 2.0 emu/cm^3 (+0.45%), whereas for an $\boldsymbol{E}$ field of −6.7 kV/cm the magnetization decreased by 3.5 emu/cm^3 (−0.77%). The effect of electric field on magnetization could be characterized by the magnetoelectric (ME) coefficient $\alpha = d\boldsymbol{M}/d\boldsymbol{E}$, which was $\sim 0.7 \times 10^{-10}$ s/cm for $\boldsymbol{E} = -6.7$ kV/cm at 100 K. This coefficient was larger than the single-phase multiferroic materials and comparable with previous work on other manganite films on piezoelectric substrate [6]. These results show the effective modulation of the magnetization by ME coupling between the manganite film and substrate through the electric field. Figure 3(b) summarizes the dependence of the change of magnetization on magnetic field during measurement at 100 K. With the increase of magnetic field, the change of the in-plane magnetization increased and tended to

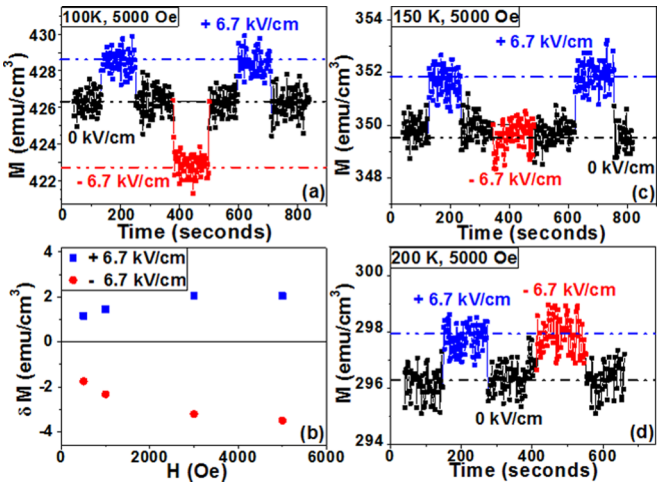

FIG. 3. (Color online) Polarization dependence of magnetization on different electric fields at (a) 100, (c) 150, and (d) 200 K with magnetic field 5000 Oe; (b) the dependence of the change of magnetization ($\delta\boldsymbol{M}$) on magnetic field at 100 K. A positive electric field of +6.7 kV/cm was applied during the cooling process from room temperature to the targeting temperature.

saturate at 5000 Oe. In order to exclude the possibility that the change of in-plane magnetization was caused by other factors such as diamagnetic PMNT substrate [33] or leakage current, the same measurements on pure PMNT substrate without PSMO film were repeated. No change of magnetization was observed in the PMNT reference sample. The effects of different electric biases on magnetization were studied using XMCD and will be discussed later.

The above magnetic measurements were conducted with an electric field of +6.7 kV/cm applied during the cooling process from room temperature to 100 K. The positive $\boldsymbol{E}$ field applied during the magnetic measurement caused the increase of magnetization while the negative field caused the decrease of magnetization. The measurements were repeated with a negative electric field, −6.7 kV/cm, applied during the cooling process (S6 in SM). The similar phenomena with opposite polarization dependence were observed, i.e., a positive $\boldsymbol{E}$ field applied during magnetic measurement decreased the magnetization while a negative field increased magnetization. These results demonstrate that the history of polarization in PMNT substrate plays an important role in controlling magnetic properties.

Figures 3(c) and 3(d) show an interesting change of magnetization with the $\boldsymbol{E}$ field at 150 and 200 K, respectively. An electric field of +6.7 kV/cm was applied during the cooling process. The negative $\boldsymbol{E}$ field did not cause any change of magnetization at 150 K. At 200 K, the negative $\boldsymbol{E}$ field increased the magnetization in the same manner shown by the positive $\boldsymbol{E}$ field. Figure 4 summarizes the temperature dependence of the change of magnetization. With the positive $\boldsymbol{E}$ field applied during measurement, the magnetization was enhanced and independent of temperature. In the case of applied negative $\boldsymbol{E}$ field during measurement, the magnetization decreased at low temperature (50 and 100 K) and then increased at high temperature (200 K).

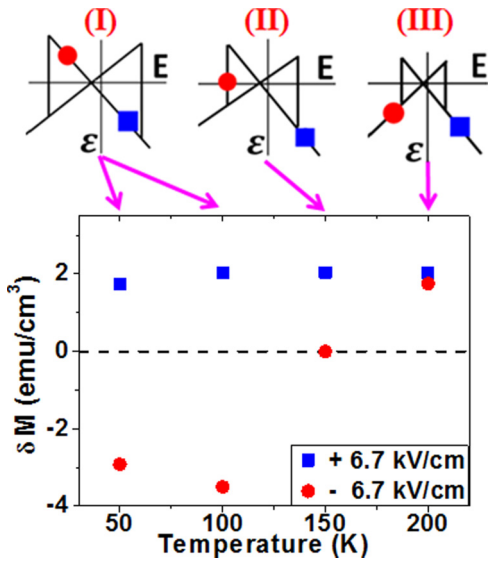

FIG. 4. (Color online) The dependence of the change of magnetization ($\delta \boldsymbol{M}$) on temperature at 5000 Oe. A positive electric field of +6.7 kV/cm was applied during the cooling process from room temperature to the targeting temperature. The upper part illustrates the response of piezoelectric PMNT to the electric field at different temperatures (three situations); the blue and red dots illustrate the position of positive and negative electric field 6.7 kV/cm, respectively.

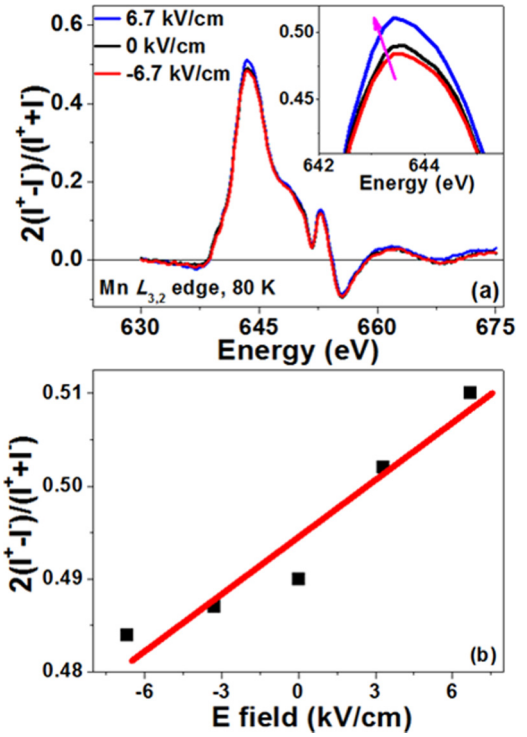

FIG. 5. (Color online) (a) Normalized XMCD measured at Mn $L_{3,2}$ with 5000 Oe magnetic field in the film plane at different electric fields on PMNT substrate. The inset is the enlarged part around the absorption region 645 eV and the arrow indicates the measurement sequence. (b) Change of peak intensity around 645 eV with applied electric field, and the line is for a viewing guide. The signals were collected in the reflectivity mode.

The electric field causes opposite strain along the out-of-plane and the in-plane directions simultaneously in (001)-oriented PMNT substrate under the assumption of conservation of unit-cell volume [6,22]. The strain occurs by small displacement of atoms in the piezoelectric [34,35]. When the temperature is decreased, a higher electric field is required to reverse the atomic displacement due to reduced thermal agitation [36]. The coercivity of the strain electric-field hysteresis loop therefore tends to increase with decreasing temperature (S7 in SM) [37]. Based on the temperature dependence of coercivity in the strain-$\boldsymbol{E}$ field loop, a model is proposed to explain the change of magnetization with strained conditions in the PSMO film.

The upper part of Fig. 4 illustrates three temperature regions (I, II, and III) with corresponding ideal butterfly loops. The positive $\boldsymbol{E}$ (blue dot) and negative $\boldsymbol{E}$ (red dot) are shown with respect to the piezoelectric coercivity in each plot. This coercivity is defined by the $\boldsymbol{E}$ value at $\varepsilon = 0$ in each butterfly loop. In region I of low temperatures (50 and 100 K), both $+\boldsymbol{E}$ and $-\boldsymbol{E}$ are assumed to be smaller than the coercivity, and $+\boldsymbol{E}$ results in the in-plane compressive strain whereas $-\boldsymbol{E}$ the in-plane tensile strain. The corresponding change of magnetization is seen in the lower part of Fig. 4. In region II (150 K), the electric field $\boldsymbol{E}$ is assumedly comparable to the piezoelectric coercivity. In such a case, the asymmetry in the butterfly loop [see Fig. 1(b) of the asymmetrical butterfly loop] from the fatigue effect [36,38] affects the induced strain at $\pm\boldsymbol{E}$, as shown in region II. The $-\boldsymbol{E}$ field did not cause any net strain in the PMNT substrate (red dot), corresponding to no change of magnetization. Due to the asymmetry of the loop, however, the $+\boldsymbol{E}$ field produces an in-plane compressive strain in the PMNT substrate (blue dot), corresponding to increased magnetization. At high temperature (200 K) corresponding to region III, the $+\boldsymbol{E}$ field is assumed to exceed the coercivity. Both the $\pm\boldsymbol{E}$ fields cause the same in-plane compressive strain in the PMNT substrate, thus transferring the same strain to the PSMO film and resulting in the same magnetization. This model generally explains that the in-plane compressive (tensile) strain increases (decreases) the magnetization. Further work on verification of this model at low temperatures would be warranted beyond this current work.

The SQUID magnetic results included the contribution from both Mn and Pr sites at low temperature [39]. In order to differentiate the element-specific magnetic contribution, XMCD, relating to the electronic structure, was employed to investigate the heterostructures. The XMCD at the Mn $\boldsymbol{L}_{3,2}$ edge (Fig. 5) and Pr $\boldsymbol{M}_{5,4}$ (S8 in SM) edge were measured at 80 K in reflectivity mode to acquire information from the film. The incident angle of x ray was 5° with respect to the film plane, and the penetration length of x ray was about 50 nm [24], which was smaller than the PSMO film thickness. The large film thickness rendered it possible to study the effects of electric field on the PSMO film only, and the contribution from the PSMO/PMNT interface was not included in the XMCD signals. The electric field affected the PSMO film through the strain mediation, as seen from the XRD results. The field of +6.7 kV/cm was applied during the cooling process from room temperature to 80 K. At the Mn $\boldsymbol{L}_{3,2}$ edge,

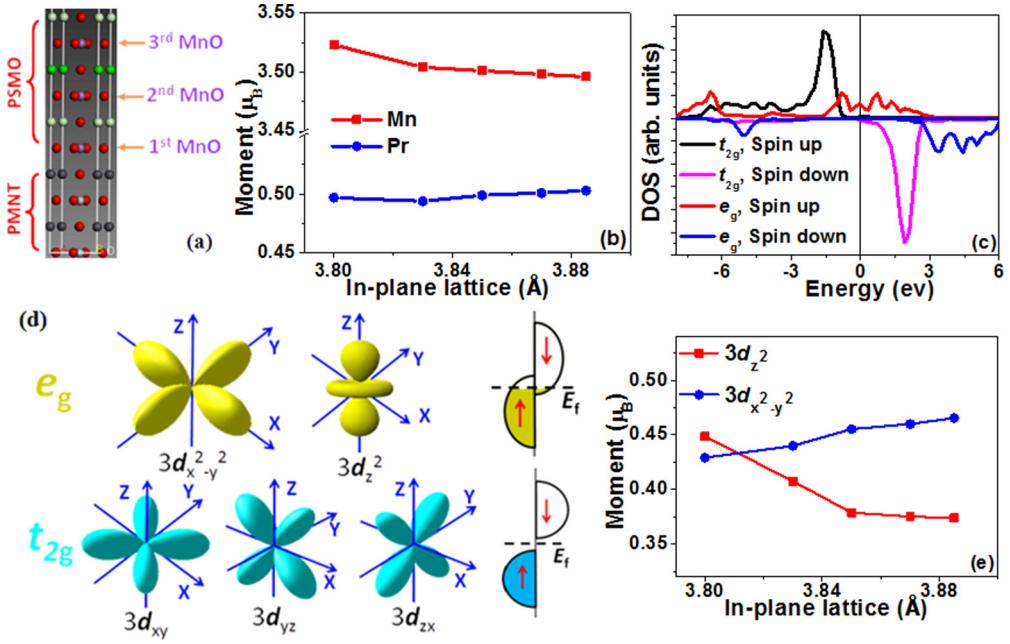

FIG. 6. (Color online) (a) The simulation configuration used in this work. (b) The calculated dependence of magnetic moment at the first Mn site and Pr site on in-plane lattice constant. (c) The calculated $3d$ DOS and (e) the magnetic spin contribution from two $\boldsymbol{e}_g$ suborbitals, at the first Mn site. (d) The illustration of $\boldsymbol{t}_{2g}$ and $\boldsymbol{e}_g$ orbitals with respect to the Fermi level $\boldsymbol{E}_f$.

$+\boldsymbol{E}$ enhanced the relative peak intensity around 645 eV of the XMCD signal. The relationship of peak intensity with the electric field is shown in Fig. 5(b), indicating the increase of magnetic moment at the Mn site with the application of positive electric field. At the Pr $\boldsymbol{M}_{5,4}$ edge, the XMCD signal was very weak, showing no obvious dependence on the electric field (S8 in SM). The effects of electric field on the trend of magnetic moment from the XMCD measurements were consistent with those from the SQUID measurement at 100 K [Fig. 3(a)]. The XMCD results indicated that the change of magnetic moment in the PSMO film under electric field arose predominantly from the Mn site, which also correlated the effects of electric field with the electronic structure of the Mn site directly. The contribution from the Pr site is therefore ignored hereafter.

First-principles simulation using the VASP package [40] was performed to study the dependence of magnetic moment on strain. The configuration used in the simulation is shown in Fig. 6(a). The electronic exchange-correlation and electron-ion interaction were described within a spin-polarized generalized-gradient approximation (GGA) and the projector augmented-wave (PAW) formalism, respectively. The plane-wave basis set with a maximum kinetic energy of 500 eV and $6 \times 6 \times 1$ k-point mesh generated by the Monkhorst-Pack scheme were adopted [41]. Although in our experiment the substrate was PMNT, the substrate composition detail was considered to be secondary in the strain-effect simulation [15]. The strain effect was studied by controlling the in-plane lattice, and structural relaxations were performed along the out-of-plane direction until the largest force between the atoms worked out to be less than 1 meV/Å.

Figure 6(b) shows the dependence of calculated magnetic moment on the in-plane lattice constant. The magnetic moment from the Mn site increased with decreasing in-plane lattice constant (increasing out-of-plane constant). No change of magnetic moment from the Pr site was obtained, consistent with the XMCD experimental results. The simulation results showed that the in-plane compressive strain increased the magnetic moment in the range around the experimental value of the in-plane lattice constant (3.86 Å), corroborating with the experimental results. This confirmed the dependence of magnetic moment of the PSMO film on electric-field-induced strain in the heterostructure. Figure 6(c) shows the calculated density of states (DOS) of the first Mn site with an in-plane lattice constant 3.85 Å. As demonstrated in Fig. 6(d), the spin-up $\boldsymbol{t}_{2g}$ band was well below the Fermi level and the spin-down $\boldsymbol{t}_{2g}$ band was well above the Fermi level. However, the $\boldsymbol{e}_g$ band had a considerable DOS around the Fermi level, indicating that the change of materials properties should be related to the electronic structure of the $\boldsymbol{e}_g$ band.

It is well known that each $3d$ orbital of Mn ions in manganite has a different anisotropy of wave function in their coupling to the surrounding oxygen ions, which is very sensitive to strain. The spin moments (the difference between the number of electrons in the majority and minority band) [42] of the two $\boldsymbol{e}_g$ orbitals were calculated. A clear dependence of magnetic moment of the two $\boldsymbol{e}_g$ orbitals on the in-plane lattice constant is seen in Fig. 6(e). With decreasing in-plane lattice constant, the spin moment contribution from $3d_z^2$ increased whereas that from $3d_{x^2-y^2}$ decreased. When the in-plane lattice decreased, the energy of $3d_{x^2-y^2}$ would become higher than that of $3d_z^2$, according to the crystal field consideration. Hence the probability to occupy $3d_{x^2-y^2}$ decreased, leading to reduced contribution to the magnetic moment. The overall contribution [red square points in Fig. 6(b)] from these two $\boldsymbol{e}_g$ orbitals was consistent with the observed experimental results. The strain-induced electron redistribution among the

two e_g orbitals was therefore responsible for the change of magnetic moment in the PSMO film in the PSMO/PMNT heterostructure under the electric field. In order to obtain more information regarding the anisotropic occupancy of $3d_{x^2-y^2}$ and $3d_z^2$ orbitals, further study involving x-ray magnetic linear dichroism (XMLD) would be warranted.

IV. SUMMARY

The electric-field control of magnetic properties of $Pr_{0.67}Sr_{0.33}MnO_3$ (PSMO) film on piezoelectric $Pb(Mg_{1/3}Nb_{2/3})O_3 - PbTiO_3$ (PMNT) substrate was investigated. The magnetic moment of the PSMO film depended on both temperature and electric biasing. The applied electric bias strained the PMNT substrate. The strain was coupled to the PSMO film in the heterostructure. The induced strain in the PSMO film showed biasing polarization dependence and temperature dependence and their corresponding effects on the PSMO magnetization. The change of magnetic moment was associated with the Mn ions. First-principles simulations showed that the strain-induced electronic redistribution of the two e_g orbitals was responsible for the change of magnetic moment. This work demonstrated that the orbital occupation probability is important for understanding the magnetoelectric effects in ferromagnetic/piezoelectric heterostructures.

ACKNOWLEDGMENTS

This research is supported by the Singapore National Research Foundation under CRP Award No. NRF-CRP10-2012-02. Use of the Advanced Photon Source (APS), an Office of Science User Facility operated for the U.S. Department of Energy (DOE) Office of Science by Argonne National Laboratory (ANL), was supported by the U.S. DOE under Contract No. DE-AC02-06CH11357. G.M.C., C.J.S., and B.Z. thank Dr. J. W. Freeland and Dr. R. A. Rosenberg for help with XMCD measurement at Sector 4, APS, ANL. Work at Brookhaven was supported by U.S. DOE-BES, Division of Materials Science and Engineering, under Contract No. DE-AC02-98CH10886.

[1] Jing Ma, Jiamian Hu, Zheng Li, and Ce-Wen Nan, Adv. Mater. **23**, 1062 (2011).
[2] W. Eerenstein, N. D. Mathur, and J. F. Scott, Nature (London) **442**, 759 (2006).
[3] K. F. Wang, J.-M. Liu, and Z. F. Ren, Adv. Phys. **58**, 321 (2009).
[4] C. A. F. Vaz, J. Hoffman, Y. Segal, J. W. Reiner, R. D. Grober, Z. Zhang, C. H. Ahn, and F. J. Walker, Phys. Rev. Lett. **104**, 127202 (2010).
[5] H. J. A. Molegraaf, J. Hoffman, C. A. F. Vaz, S. Gariglio, D. van der Marel, C. H. Ahn, and J.-M. Triscone, Adv. Mater. **21**, 3470 (2009).
[6] C. Thiele, K. Dörr, O. Bilani, J. Rödel, and L. Schultz, Phys. Rev. B **75**, 054408 (2007).
[7] P. Borisov, A. Hochstrat, X. Chen, W. Kleemann, and C. Binek, Phys. Rev. Lett. **94**, 117203 (2005).
[8] K. H. He, J. S. Chen, and Y. P. Feng, Appl. Phys. Lett. **99**, 072503 (2011).
[9] Chun-Gang Duan, S. S. Jaswal, and E. Y. Tsymbal, Phys. Rev. Lett. **97**, 047201 (2006).
[10] Y. W. Yin, J. D. Burton, Y-M. Kim, A. Y. Borisevich, S. J. Pennycook, S. M. Yang, T. W. Noh, A. Gruverman, X. G. Li, E. Y. Tsymbal, and Qi Li, Nat. Mater. **12**, 397 (2013).
[11] Wei-Gang Wang, Mingen Li, Stephen Hageman, and C. L. Chien, Nat. Mater. **11**, 64 (2012).
[12] Yoichi Shiota, Takayuki Nozaki, Frédéric Bonell, Shinichi Murakami, Teruya Shinjo, and Yoshishige Suzuki, Nat. Mater. **11**, 39 (2012).
[13] Jing Lou, Ming Liu, David Reed, Yuhang Ren, and Nian X. Sun, Adv. Mater. **21**, 4711 (2009).
[14] Ming Liu, Ziyao Zhou, Tianxiang Nan, Brandon M. Howe, Gail J. Brown, and Nian X. Sun, Adv. Mater. **25**, 1435 (2013).
[15] Hanghui Chen and Sohrab Ismail-Beigi, Phys. Rev. B **86**, 024433 (2012).
[16] J. D. Burton and E. Y. Tsymbal, Phys. Rev. B **80**, 174406 (2009).
[17] Z. G. Sheng, J. Gao, and Y. P. Sun, Phys. Rev. B **79**, 174437 (2009).
[18] C. Thiele, K. Dörr, S. Fähler, L. Schultz, D. C. Meyer, A. A. Levin, and P. Paufler, Appl. Phys. Lett. **87**, 262502 (2005).
[19] Ayan Roy Chaudhuri, S. B. Krupanidhi, P. Mandal, and A. Sundaresan, J. Appl. Phys. **106**, 054103 (2009).
[20] R. K. Zheng, Y. Jiang, Y. Wang, H. L. W. Chan, C. L. Choy, and H. S. Luo, Appl. Phys. Lett. **93**, 102904 (2008).
[21] Q. P. Chen, J. J. Yang, Y. G. Zhao, S. Zhang, J. W. Wang, M. H. Zhu, Y. Yu, X. Z. Zhang, Zhu Wang, Bin Yang, D. Xie, and T. L. Ren, Appl. Phys. Lett. **98**, 172507 (2011).
[22] L. P. Chen, F. Wang, Y. S. Chen, Y. Sun, and J. Gao, Europhys. Lett. **100**, 47006 (2012).
[23] Bangmin Zhang, Cheng-Jun Sun, Ping Yang, Wenlai Lu, Brandon L. Fisher, T. Venkatesan, Steve M. Heald, Jing-Sheng Chen, and Gan Moog Chow, Phys. Rev. B **89**, 195140 (2014).
[24] Jihwey Park, Dong Ryeol Lee, Yongseong Choi, John W. Freeland, Ki Bong Lee, Sunil K. Sihna, K. R. Nikolaev, and Allen M. Goldman, Appl. Phys. Lett. **95**, 102504 (2009).
[25] See Supplemental Material at http://link.aps.org/supplemental/10.1103/PhysRevB.91.174431 for the illustration of sample configuration with electric bias, volume conservation, rocking curve and magnetization-temperature curve of PSMO film, magnetostriction effect, effects of electric field on magnetization with negative bias during cooling, temperature dependence of coercivity of PMNT, and Pr $M_{5,4}$ edge XMCD with different electric field.
[26] Seung-Eek Park and Thomas R. Shrout, J. Appl. Phys. **82**, 1804 (1997).
[27] Ian MacLarena, Zhong Lin Wang, H. S. Wang, and Qi Li, Appl. Phys. Lett. **80**, 1406 (2002).
[28] Bangmin Zhang, Jingsheng Chen, and Gan Moog Chow, IEEE Trans. Magn. **47**, 4402 (2011).
[29] Ashok Rao, P. Poornesh, K. K. Wu, Y. K. Kuo, and S. K. Agarwal, Solid State Commun. **172**, 54 (2013).

[30] X. W. Wu, M. S. Rzchowski, H. S. Wang, and Qi Li, Phys. Rev. B **61**, 501 (2000).
[31] H. S. Wang, Qi Li, Kai Liu, and C. L. Chien, Appl. Phys. Lett. **74**, 2212 (1999).
[32] G. Lalitha and P. Venugopal Reddy, Ultrasonics **52**, 706 (2012).
[33] Jang-Yong Kim, Lide Yao, and Sebastiaan van Dijken, J. Phys.: Condens. Matter **25**, 082205 (2013).
[34] Boris A. Strukov and Arkadi P. Levanyuk, *Ferroelectric Phenomena in Crystals* (Springer, New York, 1998), p. 35.
[35] I-Wei Chen and Ying Wang, Ferroelectrics **206**, 245 (1998).
[36] Hong Wang, Tadashi Matsunaga, Hua-Tay Lin, and Alexander M. Mottern, Smart Mater. Struct. **21**, 025009 (2012).
[37] Xiuli Zhang, Haisheng Xu, and Yanni Zhang, J. Phys. D: Appl. Phys. **44**, 155501 (2011).
[38] W. L. Warren, B. A. Tuttle, and D. Dimos, Appl. Phys. Lett. **67**, 1426 (1995).
[39] J.-G. Park, M. S. Kim, H.-C. Ri, K. H. Kim, T. W. Noh, and S.-W. Cheong, Phys. Rev. B **60**, 14804 (1999).
[40] G. Kresse and J. Hafner. Phys. Rev. B **47**, 558 (1993).
[41] G. Kresse and D. Joubert, Phys. Rev. B **59**, 1758 (1999).
[42] J. Stohr, J. Magn. Magn. Mater **200**, 470 (1999).